NOTES AND CORRESPONDENCE

Oceanic Turbulence Dissipation Measurements in SWADE

W. M. DRENNAN AND M. A. DONELAN

National Water Research Institute, Burlington, Ontario, Canada

E. A. TERRAY

Woods Hole Oceanographic Institution, Woods Hole, Massachusetts

K. B. KATSAROS

University of Washington, Seattle, Washington

1 March 1995 and 10 October 1995

ABSTRACT

Recent experiments measuring turbulence dissipation rates in the upper ocean can be divided into two types: those supporting an analogy between the upper ocean and lower atmosphere, with dissipation rates following wall layer behavior, and those finding oceanic dissipation rates to be much higher than wall layer predictions. In an attempt to reconcile these two diverse sets of observations, Terray et al. proposed a wave-dependent scaling of the dissipation rate based on the significant wave height and the rate of energy input from the wind to the waves. Their parameterization was derived from observations of strongly forced, fetch-limited waves, although they conjectured that it would apply in typical oceanic conditions as well. This paper reports new measurements of turbulent kinetic energy dissipation made in the North Atlantic Ocean from a SWATH ship during the recent Surface Waves Dynamics Experiment (SWADE). These data support the scaling of Terray et al., verifying its validity when applied to the more fully developed waves typical of the ocean.

1. Introduction

The rate of turbulent kinetic energy dissipation in the upper ocean is an important parameter for the modeling of mixed layer processes. Although determining its vertical distribution has been the goal of many studies during the last 30 years, recent evidence has questioned even the order of magnitude of the dissipation rates found in earlier work.

The studies of Stewart and Grant (1962), Arsenyev et al. (1975), Dillon et al. (1981), Oakey and Elliot (1981), Jones (1985), and Soloviev et al. (1988) liken the upper ocean to a classical wall layer, where the turbulence is generated solely by the working of Reynolds stresses on the mean shear. In this view, the dissipation rates ϵ in both the upper ocean and lower atmosphere behave in the same way, depending only on the friction velocity u_*, the distance from the interface z, and von Kármán's constant κ; namely, $\epsilon = u_*^3/\kappa z$. Support for this wall layer behavior (to within a factor of 5) was found in each of the studies reported above, leading one paper (i.e., Soloviev et al.) to conclude that shear is indeed the only significant source of turbulent energy in the upper ocean and that waves are not an important factor in the problem.

This view, however, was challenged by Kitaigorodskii et al. (1983), who, in a series of tower data recorded in strongly forced, fetch limited conditions, found dissipation rates one to two orders of magnitude above wall layer predictions. They proposed that energy input from wave breaking was responsible for the large dissipation values they observed. Recently, other experiments (Gregg 1987; Gargett 1989; Agrawal et al. 1992; Osborn et al. 1992; Anis and Moum 1992; Terray et al. 1996), again with near-surface measurements in strongly forced conditions, have supported Kitaigorodskii et al. in finding enhanced dissipation rates. We note here that the bulk of the earlier studies were conducted either in lighter winds or deeper in the water column than more recent work and therefore that the effects of wave breaking would be considerably less pronounced. Taken together, these studies point to a profound difference in the surface-layer dynamics of

Corresponding author address: Dr. M. A. Donelan, National Water Research Institute, Canada Centre for Inland Waters, P.O. Box 5050, Burlington, ON L7R 4A6, Canada.

the ocean and atmosphere due to the pronounced effect of breaking surface waves on the oceanic boundary layer.

The model of Terray et al. (1996) was proposed to resolve the differences between the two conflicting groups of data. Wave effects are included in the model through the introduction of wave-related variables H_s, k_p, c_p, and F into the dimensional analysis. Here H_s is the significant height (four times the rms height) of the wind sea, k_p and c_p the wavenumber and phase velocity at the wind sea peak frequency, and $\rho_w F$ the rate of energy input from the wind to the waves, where ρ_w is the water density. Here F is calculated by integrating the growth rate $\beta(\omega, \theta)$ (Donelan and Pierson 1987) over the frequency–direction spectrum $S_\eta(\omega, \theta)$ of the waves

$$F = g \int \beta S_\eta d\omega d\theta. \tag{1}$$

With this expanded set of variables, the dissipation rate can be expressed as

$$\frac{\epsilon H_s}{F} = f\left(\frac{z}{H_s}, \frac{c_p}{u_{*a}}, \frac{F}{u_{*a}^2 c_p}, k_p H_s\right). \tag{2}$$

Noting that the last two variables can be parameterized as functions of wave age, c_p/u_{*a} (Donelan et al. 1985), they may be eliminated from the problem so that

$$\frac{\epsilon H_s}{F} = f\left(\frac{z}{H_s}, \frac{c_p}{u_{*a}}\right). \tag{3}$$

Throughout, the subscripts a and w on the friction velocity refer to the air and water sides.

Based on an extensive set of tower-based data collected using acoustic, mechanical, and laser Doppler velocimeters during the WAVES experiment in Lake Ontario, Terray et al. (1996) proposed the existence of an intermediate range of depths, $z_b < z < z_t$, in which the dependence of the dissipation rate on wave age is manifested entirely through its dependence on the scaling variables H_s and F. Although the relation (3) indicates a possible explicit wave age dependence of the dissipation rate, this was not supported by the WAVES data. In this layer, it was found that

$$\epsilon H_s / F = 0.3(z/H_s)^{-2}. \tag{4}$$

To enforce consistency with the observations of wall layer scaling at sufficient depths, they matched the above expression to the wall layer form of the dissipation at z_t, obtaining $z_t/H_s = 3.6(\bar{c}/u_{*a})$, where $F \equiv u_{*w}^2 \bar{c}$. The upper limit, z_b, of the intermediate range (4) was obtained by assuming that the dissipation rate above z_b is constant. This idea is consistent with the introduction of H_s as an imposed length scale for the turbulence initially generated by breaking. With this assumption, they were able to calculate z_b by equating the vertically integrated dissipation in the water to the wind input, F, at the surface, obtaining $z_b/H_s = 0.6$.

As mentioned earlier, the intermediate depth scaling proposed by Terray et al. was based on a dataset that was restricted to young waves with ages in the range $c_p/u_{*a} \approx 4$–7 (equivalently $U/c_p \approx 3$–4), and therefore its applicability to typical oceanic conditions where the waves are relatively more mature is open to question. Furthermore, their observations were almost entirely from the intermediate layer $z_b < z < z_t$, with only four values (representing two runs) at lesser depths, and consequently their arguments establishing the thickness of the region having $\epsilon \propto z^{-2}$ remain to be tested.

It was with these questions in mind that supplementary dissipation measurements were undertaken as part of the Surface Waves Dynamics Experiment (SWADE). Details of the measurements and analysis techniques are discussed in sections 2 and 3. Results are then presented in section 4, and conclusions in section 5.

2. The experiment

The measurements presented herein were taken as part of SWADE, which took place between October 1990 and March 1991. For a detailed description of the SWADE objectives and plan see Weller et al. (1991). High-resolution measurements near the air–sea interface were obtained using a SWATH (small water-plane area, twin hull) ship, the *Frederick G. Creed.* The *Frederick G. Creed* is 20 m long by 10 m wide and has a well-streamlined superstructure—see Fig. 1. Buoyancy is provided by two 2-m diameter pontoons located about 2 m below the waterline and attached to the hull by two narrow struts running the length of the ship. By design the ship has a small surface-piercing area, making it an excellent platform for air–sea research. The *Creed* operated off the Maryland coast (see Fig. 2) during two intensive operating periods, IOP2 and IOP3, each of two weeks duration.

A variety of surface and near-surface measurements were made from the *Creed,* including directional wave spectra from a six-element wave wire array (Drennan et al. 1994); eddy-correlation measurements of the atmospheric fluxes of momentum, heat, and water vapor (Katsaros et al. 1993); and near-surface current measurements. To successfully make these measurements from a moving platform, such as a ship, the six degrees of motion of the platform (i.e., pitch, roll, yaw, heave, surge, and sway) must be recorded at each instant and these signals used to correct the various time series. The algorithms for doing so are described by Drennan et al. (1994) and Anctil et al. (1994) for the wave gauges and velocity sensors, respectively.

The wave gauge array was positioned two meters in front of the bow of the *Creed,* between the two hulls, and well ahead of any surface disturbances created by

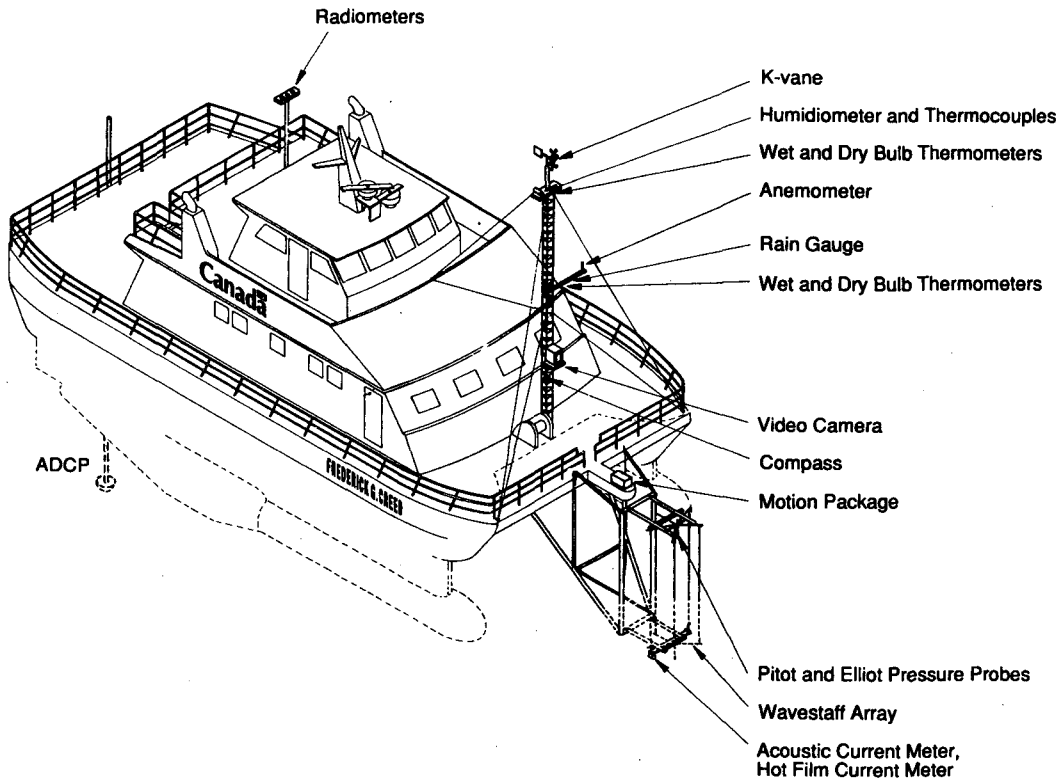

FIG. 1. Illustration of the SWATH ship *Frederick G. Creed* showing the equipment deployed during SWADE.

the ship. The dissipation measurements reported here were obtained from an acoustic travel-time current meter, the Minilab SD-12 (Sensordata A/S, Bergen, Norway), which was installed immediately below one of the wave staffs, nominally 2 m below the surface. The current meter was approximately 3 m ahead of and 2.5 m to the side of one of the pontoons. The SD-12 is a three axis device, with two orthogonal components of velocity being measured in the same volume (along folded paths approximately 3 cm in length) and the third component measured in a volume offset by 3–4 cm. The current meter was mounted so that the paired components were at 45° to the vertical and bow–stern axes. In order to use the SD-12 for the present experiment, a 1.5-Hz 3-dB RC filter was removed and replaced with a 5-Hz 3-dB RC filter. All channels were sampled at a rate of 20 Hz, and the effects of the filter transfer function were removed during the analysis. The current meter was calibrated for gain in the National Water Research Institute's 100-m towing tank prior to deployment, and the offsets of the instrument were measured during a prelaunch "bucket" zero. Unfortunately a postfield calibration was not possible because the bow array and current meter were lost at sea during the third intensive operating period, IOP3.

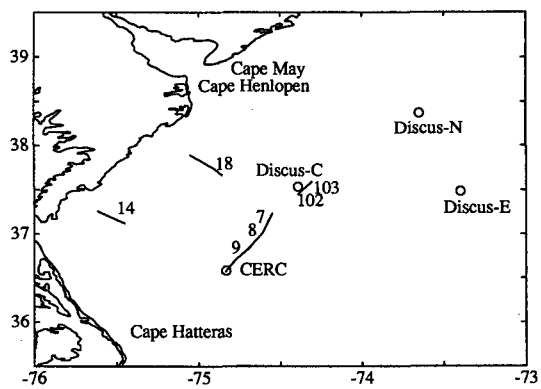

FIG. 2. Map showing the location and track of the *Frederick G. Creed* during the SWADE dissipation runs. The numbers correspond to runs listed in Table 1. Circles mark the location of the four 3-m discus buoys deployed during SWADE.

3. Analysis

The rates of kinetic energy dissipation were calculated from the inertial subranges of the velocity spectra following Kolmogorov's dimensional argument that in these ranges

$$E_1(k) = \frac{18}{55} C\epsilon^{2/3} k^{-5/3}, \qquad (5)$$

where E_1 is the one-dimensional longitudinal velocity spectrum and C is a constant (Monin and Yaglom 1975, section 23.3). Because the turbulent velocities are an order of magnitude smaller than the advection velocity (i.e., ship plus current velocities), we can apply Taylor's frozen turbulence hypothesis to convert frequency spectra to wavenumber space, via the mapping $\omega = U_d k$, as

$$S_1(\omega) = \frac{18}{55} C\epsilon^{2/3} U_d^{2/3} \omega^{-5/3}, \qquad (6)$$

where U_d is the velocity at which the turbulence convects (or drifts) past the probe. The Kolmogorov constant, C in Eqs. (5)–(6), is taken here to be 1.5 for horizontal and 2.0 (4/3 × 1.5) for vertical velocity spectra.

In our analysis, only inertial subrange levels at frequencies above that of the wave peak are used because turbulent velocities at these frequencies are not affected by the unsteady ship motion. Figure 3 shows examples of both uncorrected and motion-corrected (Anctil et al. 1994) spectra. We note that whereas we were able to apply Taylor's hypothesis in its conventional form, taking U_d to be the mean velocity, Terray et al. (1996) in their tower-based experiment experienced comparatively small mean currents and therefore used an extension of Taylor's hypothesis to unsteady advection given by Lumley and Terray (1983).

In order to use the model of Terray et al., several other measured or calculated values are required: H_s and F are calculated from the surface elevation spectra, which themselves are determined from the wave gauge signals after correction for the unsteady ship motion. In calculating F using (1), either the directional wave height spectrum $S_\eta(\omega, \theta)$ estimated as per Drennan et al. (1994) or, when necessary, the 1D frequency spectrum $S_\eta(\omega)$ was used. In the latter cases (during a few runs, only a single wave staff was functioning) the frequency spectra were first corrected for the Doppler shifting of the frequencies due to the motion of the ship, and then the angular integrations carried out assuming the $\mathrm{sech}^2(\alpha\theta)$ directional distribution proposed by Donelan et al. (1985). We note here that H_s refers to the significant height of the *wind sea* only. The *Creed* was equipped with a *K*-Gill anemometer vane, mounted at 12 m above the foredeck. Following the procedure outlined by Katsaros et al. (1993) and Anctil et al. (1994), the measured horizontal and vertical wind velocities were corrected to account for the motion of the ship and the friction velocity u_{*a} calculated directly using the eddy correlation method. We calculated the friction velocity in the water, u_{*w}, from an assumed stress balance across the interface (i.e., $\rho_w u_{*w}^2 = \rho_a u_{*a}^2$).

4. Results

We present the results from 20 runs (of 17.5 min), where the wave age (U/c_p) ranged from 1.1 to 2, H_s from 1 to 3 m, and the wind speed from 8 to 12 m s^{-1}—see Table 1. The approximate location and heading of the *Creed* during each run can be seen in Fig. 2. In each of these runs, the *Creed* was cruising into the wind. A further 25 runs were rejected due to either missing meteorological data (12 runs) or high noise levels (13 runs). Variations in the inertial subrange of the velocity spectra allow us to estimate the uncertainties in estimates of ϵ. Ninety-five percent (2σ) confidence limits yield error bands of, on average, ±36%, or in the worst case, ±63%. These uncertainties are in addition to those inherent in the value of the Kolmogorov constant (see Monin and Yaglom 1975). Directional wave spectra indicate a simple wind sea in 18 of the cases, with a cross swell running at 60 to 90 degrees from the wind sea in the other 2. These latter 2 runs are indicated in Table 1 with a dagger. We note here that in the first 10 runs, in Table 1, the depths z may be up to 10% (20 cm) in error.

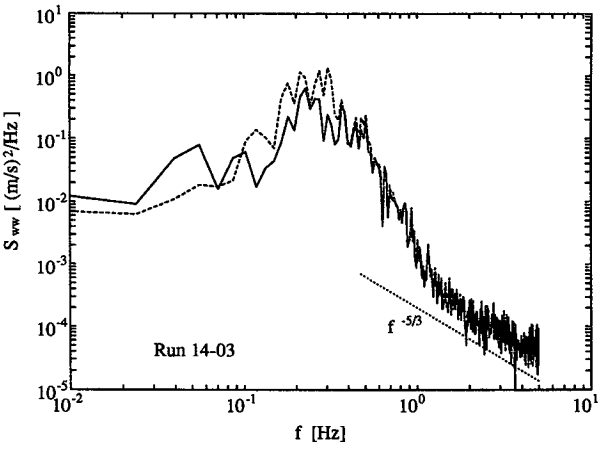

FIG. 3. Vertical velocity frequency spectra S_{ww} for run 14-03. The dashed and solid lines refer to the direct current meter and motion-corrected velocities respectively. The dotted line shows the expected $f^{-5/3}$ slope of the inertial subrange.

The dissipation rates, ϵ_u and ϵ_w, calculated respectively from the longitudinal and vertical velocities, are shown in Table 1. Also shown is $\epsilon_{\text{wall}} = u_{*w}^3/\kappa z$, the wall layer estimates of dissipation rate, with von Kármán's constant κ taken to be 0.4. In Fig. 4, we plot both the SWADE and WAVES data in the wall layer coordinates of Soloviev et al. (1988). In these coordinates, dissipation rates in agreement with wall layer theory fall on the vertical line $\epsilon\kappa z/u_{*w}^3 = 1$. In all cases, the measured dissipation rates in SWADE are seen to be one to two orders of magnitude higher than wall layer theory predicts. More importantly, whereas the SWADE data are typically taken at greater depths than the WAVES data (i.e., larger gz/u_{*w}^2 for similar friction velocities) they show *larger normalized dissipation rates!* These features clearly illustrate the inadequacy of wall layer theory in the near-surface region.

TABLE 1. Data summary. Symbols are JD: Julian day, H_s: significant wave height (4 × rms wave height), D: water depth, z: current meter depth, U_d: advection velocity (ship speed), U_d/U_{rms}: ratio of ship speed to rms wave velocity, f_p: wave peak frequency, U_{12}: windspeed at 12 m; U/c_p, u_{*a}/c_p: inverse wave ages; u_{*w}: water side friction velocity; F: rate of energy input from wind to sea per unit density; ϵ_{wall}, ϵ_u, ϵ_w: dissipation rates via wall layer theory, horizontal velocity spectra, and vertical velocity spectra. The runs identified with the dagger had cross swells of about 40% and 50% H_s respectively.

Run	JD/time UTC	H_s (m)	D (m)	z (m)	U_d (m s^{-1})	U_d/U_{rms}	f_p (Hz)	U_{12} (m s^{-1})	U/c_p	u_{*a}/c_p	u_{*w} (m s^{-1})	$10^4\ F$ [(m s^{-1})^3]	$10^4\ \epsilon_{\text{wall}}$ (m^2 s^{-3})	$10^4\ \epsilon_u$ (m^2 s^{-3})	$10^4\ \epsilon_w$ (m^2 s^{-3})
7-05	019/2235	0.88	339	1.81	2.13	10.80	0.29	10.45	1.94	0.074	0.0135	2.50	.034	0.31	0.17
8-01	020/0015	0.99	109	1.79	2.44	10.68	0.28	10.00	1.80	0.061	0.0115	2.21	.021	0.40	0.35
8-03	020/0032	0.95	109	1.78	2.44	10.89	0.29	9.97	1.85	0.067	0.0121	2.26	.025	0.34	0.31
8-05	020/0050	0.95	109	1.78	2.45	10.58	0.26	9.60	1.60	0.066	0.0131	2.51	.032	0.44	0.29
8-07	020/0107	0.95	109	1.78	2.46	10.51	0.26	9.46	1.58	0.053	0.0108	1.63	.018	0.30	0.36
8-09	020/0124	0.91	109	1.77	2.47	10.53	0.26	9.00	1.50	0.053	0.0108	1.58	.018	0.24	0.36
9-02	020/0325	1.03	73	1.73	2.59	8.47	0.24	8.91	1.37	0.049	0.0105	1.21	.017	1.05	1.31
9-04	020/0342	1.05	73	1.74	2.60	9.42	0.24	8.83	1.36	0.043	0.0094	1.10	.012	0.48	0.54
9-06	020/0400	1.05	73	1.74	2.60	9.20	0.26	8.46	1.41	0.043	0.0088	0.96	.010	0.28	0.20
9-08	020/0417	1.11	73	1.74	2.61	9.10	0.24	8.16	1.26	0.042	0.0091	0.78	.011	0.36	0.25
14-03	022/0007	1.39	20	1.44	1.95	4.55	0.18	11.24	1.31	0.054	0.0155	4.92	.084	2.16	0.72
14-05	022/0024	1.61	20	1.25	1.86	3.80	0.18	11.67	1.36	0.058	0.0169	5.23	.097	2.72	1.23
14-07	022/0042	1.72	20	1.27	1.85	3.83	0.18	11.99	1.40	0.057	0.0165	5.66	.088	5.41	2.31
14-09	022/0059	1.61	20	1.29	1.87	4.25	0.19	11.86	1.45	0.064	0.0175	5.36	.104	2.48	1.31
14-11	022/0117	1.62	20	1.32	1.85	4.01	0.18	11.27	1.31	0.059	0.0172	6.42	.096	3.73	1.13
18-01	022/1740	2.17	30	1.84	1.87	3.65	0.17	10.11	1.10	0.052	0.0162	4.57	.058	2.90	1.38
18-03	022/1757	2.04	30	1.89	1.90	4.03	0.16	10.49	1.08	0.059	0.0192	6.08	.094	4.27	1.20
18-09	022/1849	1.88	27	1.84	1.90	4.70	0.18	9.95	1.15	0.058	0.0169	5.23	.066	3.02	2.35
102-03†	056/1727	2.34	185	1.44	1.58	2.85	0.16	10.67	1.09	0.035	0.0115	2.35	.026	3.88	3.87
103-01†	056/1759	2.62	180	1.85	1.60	3.06	0.18	9.54	1.10	0.047	0.0136	2.89	.034	1.88	1.28

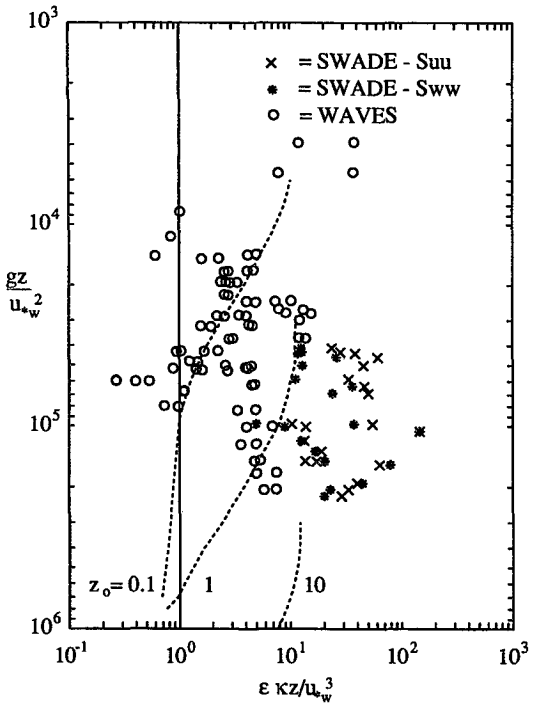

FIG. 4. Dissipation rate vs depth in the wall layer coordinates of Soloviev et al. (1988). The vertical line represents the result of wall layer theory: $\epsilon = u_{*w}^3/\kappa z$. The three dashed lines represent the predictions from the model of Craig and Banner (1994) for roughness lengths of 0.1, 1.0, and 10 m with $\alpha = 100$. Other parameters in the Craig and Banner model are as in their Table 1.

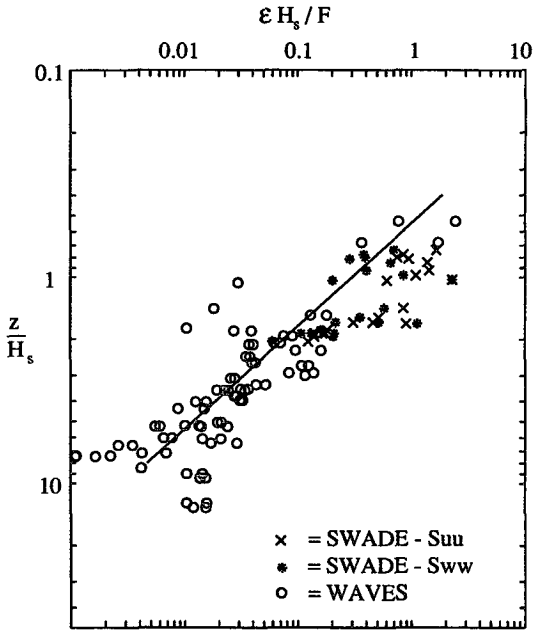

FIG. 5. Dissipation rate vs depth in the scaled coordinates of Terray et al. (1996). The line represents the best fit of the WAVES data: $\epsilon H_s/F = 0.3(z/H_s)^{-2}$. Note that the SWADE data grouped around $z/H_s \approx 2$ have a depth (z) uncertainty of about 10% (see text).

We plot the dissipation measured in both SWADE (Table 1) and WAVES using the wave-dependent scaling of Terray et al. (1996) [i.e., Eqs. (3) and (4)] in Fig. 5. In these coordinates the two datasets fall on a single curve, supporting the validity of the scaling over a wide range of significant heights and wave development (recall that WAVES had $H_s \approx 0.2 - 0.3$ m and $c_p/u_{*a} \approx 4 - 7$, whereas in SWADE $H_s \approx 0.9 - 2.6$ m and $c_p/u_{*a} \approx 13 - 29$).

A key point in the argument of Terray et al. (1996), embodied in our Eq. (3), is that when properly scaled, the dissipation in the intermediate layer reduces to a function solely of the nondimensional depth. However, as pointed out by those authors, their use of significant height as a scale for depth was made on physical grounds, it being associated with the depth of turbulent energy penetration into the water column during breaking events (Rapp and Melville 1990), and an alternate choice in terms of the wavenumber at the peak of the wind sea spectrum k_p cannot be excluded on logical grounds. We have plotted the data of Fig. 5 again in Fig. 6, scaled on k_p and F, and find that the data collapse as well in terms of these quantities. Because the significant slope can be expressed as $k_pH_s = 0.9(u_{*a}/c_p)^{0.5}$ (Maat et al. 1991), only a weak residual wave-age dependence is introduced into Eq. (3) by the wrong choice of length scale, and therefore it is not possible to discriminate between the two possibilities on the basis of the SWADE data. However, the use of k_p has a practical advantage. As pointed out above, H_s refers to

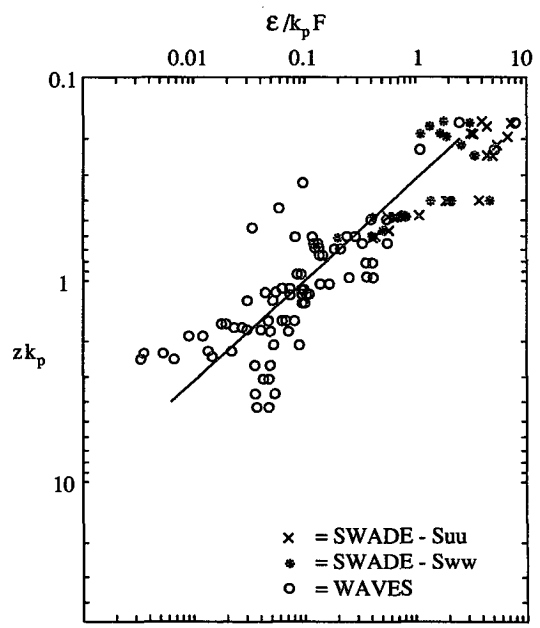

FIG. 6. Dissipation rate vs depth in the scaled coordinates ϵ/k_pF vs zk_p. The line represents $\epsilon/k_pF = 0.1(zk_p)^{-2}$.

the significant wave height of the *wind sea.* For the WAVES dataset this was equal to the measured significant height. More generally, however, swell and wind sea coexist, making it difficult to estimate the appropriate value of H_s, whereas k_p is more easily estimated from the wave spectrum.

Finally, we discuss briefly the recent attempt by Craig and Banner (1994) to model the dynamics of the near-surface region using a low-order turbulence closure model. Expanding somewhat on conventional practice in modeling shear flows over rough boundaries, they express the turbulence length scale in terms of a roughness length z_0 as $l = \kappa(z_0 + z)$ (note that we use coordinates in which the fluid occupies $z > 0$). Close to the surface, roughly for $z \leq 6z_0$, Craig and Banner find that

$$\epsilon = 2.4\alpha u_{*w}^3 z_0^{2.4}(z_0 + z)^{-3.4}, \qquad (7)$$

where αu_{*w}^3 is the kinetic energy flux at the surface. Taking α to be a constant, $\alpha = 100$, and roughness lengths in the range 0.1 to 1 m, Craig and Banner found that their model could be made to agree qualitatively with much of the data of Agrawal et al. (1992) and Osborn et al. (1992), although the data of Anis and Moum (1992) required $z_0 \sim 8$ m. They conjectured that the rather large value of z_0 required in the latter case indicated a failure of the model due to the presence of swell.

We plot the model results of Craig and Banner for $\alpha = 100$ and roughness lengths of 0.1, 1 m (taken from their Fig. 7 using parameter values from their Table 1), and 10 m [the latter using Eq. (7) above] in Fig. 4, together with both WAVES and SWADE data. From the figure, it is apparent that the SWADE data do not support the Craig and Banner model as implemented with constant α: the measured dissipation rates are up to ten times higher than predicted. However, if αu_{*w}^3 is taken to be the wind input F [cf. Eq. (1)] as suggested by Terray et al. (1996), then α becomes wave age dependent. The values of α in SWADE are then approximately double those of WAVES, leading to a doubling of the predicted dissipation rates. With these larger values of α, the roughness lengths required to get a reasonable agreement with the SWADE data are in the range of 1 to 3 m—approximately equal to the significant wave height.

5. Conclusions

The oceanic data collected during the SWADE campaign yield dissipation rates in the near-surface region that are far higher than would be generated in a wall-bounded shear layer, exceeding wall layer predictions by one to two orders of magnitude. Our results support the wave-dependent scaling of Terray et al. (1996), thereby extending it to the more fully developed conditions typical of the ocean and are consistent with their conjecture of an intermediate range of depths over which the scaled dissipation is inversely proportional to the nondimensional depth squared. These results illustrate the importance of wave breaking in the dynamics of the upper ocean and highlight the fundamental difference between the atmospheric and oceanic surface boundary layers.

Acknowledgments. We gratefully acknowledge the support for SWADE provided by the U.S. Office of Naval Research (Grants N0014-88-J-1028 and N0014-94-1-0629 to the National Water Research Institute and Grant N0014-89-1785 to the University of Washington). Support for the use of the SWATH ship was provided by the Office of Naval Research, the National Aeronautics and Space Administration, the Coastal Engineering Research Center of the U.S. Army, Environment Canada, and the Canadian Department of Fisheries and Oceans. E.A.T. acknowledges support from the National Science Foundation (Grant OCE-93-01440).

REFERENCES

Agrawal, Y. C., E. A. Terray, M. A. Donelan, P. A. Hwang, A. J. Williams III, W. M. Drennan, K. K. Kahma, and S. A. Kitaigorodskii, 1992: Enhanced dissipation of kinetic energy beneath surface waves. *Nature,* **359,** 219–220.

Anctil, F., M. A. Donelan, W. M. Drennan, and H. C. Graber, 1994: Eddy correlation measurements of air–sea fluxes from a Discus buoy. *J. Atmos. Oceanic Technol.,* **11,** 1144–1150.

Anis, A., and J. N. Moum, 1992: The superadiabatic surface layer of the ocean during convection. *J. Phys. Oceanogr.,* **22,** 1221–1227.

Arsenyev, S. A., S. V. Dobroklonsky, R. M. Mamedov, and N. K. Shelkovnikov, 1975: Direct measurements of some characteristics of fine-scale turbulence from a stationary platform in the open sea. *Izv. Atmos. Ocean. Phys.,* **11,** 530–533.

Craig, P. D., and M. L. Banner, 1994: Modeling wave-enhanced turbulence in the ocean surface layer. *J. Phys. Oceanogr.,* **24,** 2546–2559.

Dillon, T. M., J. G. Richman, C. G. Hansen, and M. D. Pearson, 1981: Near-surface turbulence measurements in a lake. *Nature,* **290,** 390–392.

Donelan, M. A., and W. J. Pierson, 1987: Radar scattering and equilibrium ranges in wind generated waves with applications to scatterometry. *J. Geophys. Res.,* **92,** 4971–5029.

——, J. Hamilton, and W. H. Hui, 1985: Directional spectra of wind-generated waves. *Philos. Trans. Roy. Soc. London,* **A315,** 509–562.

Drennan, W. M., M. A. Donelan, N. Madsen, K. B. Katsaros, E. A. Terray, and C. N. Flagg, 1994: Directional wave spectra from a Swath ship at sea. *J. Atmos. Oceanic Technol.,* **11,** 1109–1116.

Gargett, A. E., 1989: Ocean turbulence. *Ann. Rev. Fluid Mech.,* **21,** 419–451.

Gregg, M. C., 1987: Structures and fluxes in a deep convecting mixed layer. *Dynamics of the Ocean Mixed Layer,* P. Müller and D. Henderson, Eds., Hawaiian Institute of Geophysics, 1–23.

Jones, I. S. F., 1985: Turbulence below wind waves. *The Ocean Surface—Wave Breaking, Turbulent Mixing and Radio Probing,* Y. Toba and H. Mitsuyasu, Eds., Reidel, 437–442.

Katsaros, K. B., M. A. Donelan, and W. M. Drennan, 1993: Flux measurements from a Swath ship in SWADE. *J. Mar. Sys.,* **4,** 117–132.

Kitaigorodskii, S. A., M. A. Donelan, J. L. Lumley, and E. A. Terray, 1983: Wave-turbulence interactions in the upper ocean: Part II. *J. Phys. Oceanogr.,* **13,** 1988–1999.

Lumley, J. L., and E. A. Terray, 1983: Kinematics of turbulence convected by a random wave field. *J. Phys. Oceanogr.*, **13,** 2000–2007.

Maat, N., C. Kraan, and W. A. Oost, 1991: The roughness of wind waves. *Bound.-Layer Meteor.*, **54,** 89–103.

Monin, A. S., and A. M. Yaglom, 1975: *Statistical Fluid Mechanics.* Vol. II. The MIT Press, 874 pp.

Oakey, N. S., and J. A. Elliott, 1982: Dissipation within surface mixed layer. *J. Phys. Oceanogr.*, **12,** 171–185.

Osborn, T., D. M. Farmer, S. Vagle, S. Thorpe, and M. Cure, 1992: Measurements of bubble plumes and turbulence from a submarine. *Atmos.–Ocean,* **30,** 419–440.

Rapp, R. J., and W. K. Melville, 1990: Laboratory measurements of deep-water breaking waves. *Philos. Trans. Roy. Soc. London,* **A331,** 735–800.

Soloviev, A. V., N. V. Vershinsky, and V. A. Bezverchnii, 1988: Small-scale turbulence measurements in the thin surface layer of the ocean. *Deep-Sea Res.*, **35,** 1859–1874.

Stewart, R. W., and H. L. Grant, 1962: Determination of the rate of dissipation of turbulent energy near the sea surface in the presence of waves. *J. Geophys. Res.*, **67,** 3177–3180.

Terray, E. A., M. A. Donelan, Y. C. Agrawal, W. M. Drennan, K. K. Kahma, A. J. Williams III, P. A. Hwang, and S. A. Kitaigorodskii, 1996: Estimates of kinetic energy dissipation under breaking waves. *J. Phys. Oceanogr.*, **26,** 792–807.

Weller, R. A., M. A. Donelan, M. G. Briscoe, and N. E. Huang, 1991: Riding the crest: A tale of two wave experiments. *Bull. Amer. Meteor. Soc.*, **72,** 163–183.